



Lentiviral vector delivery of short hairpin RNA to NG2 and neurotrophin-3 promotes locomotor recovery in injured rat spinal cord

Title	Lentiviral vector delivery of short hairpin RNA to NG2 and neurotrophin-3 promotes locomotor recovery in injured rat spinal cord
Author(s)	Donnelly, Eleanor M.;Madigan, Nicolas N.;Rooney, Gemma E.;Knight, Andrew;Chen, Bingkun;Ball, Bret;Kinnavane, Lisa;Garcia, Yolanda;Dockery, Peter;Fraher, John;Strappe, Padraig M.;Windebank, Anthony J.;O'Brien, Timothy;McMahon, Siobhan S.
Publication Date	2012-01-08
Publisher	Elsevier
Repository DOI	10.3109/14653249.2012.714865

Lentiviral vector delivery of shRNA to NG2 and Neurotrophin-3 promotes locomotor recovery in injured rat spinal cord

Eleanor M. Donnelly (1), Nicolas N. Madigan (1, 2), Gemma E. Rooney (2), Andrew Knight (2), Bingkun Chen (2), Bret Ball (2), Lisa Kinnavane (3), Yolanda Garcia (3), Peter Dockery (3), John Fraher (4), Padraig M. Strappe (5), Anthony J. Windebank (2), Timothy O'Brien (1), Siobhan S. McMahon (3 *)

(1) Regenerative Medicine Institute, NUI Galway, Ireland.

(2) Department of Neurology, Mayo Clinic, Rochester, MN, USA

(3) Discipline of Anatomy, NUI Galway, Ireland

(4) Department of Anatomy, University College Cork, Ireland

(5) School of Biomedical Sciences, Charles Sturt University, Australia

***Corresponding author**

Dr Siobhan McMahon, Discipline of Anatomy, NUI Galway, Ireland.

Email: siobhan.mcmahon@nuigalway.ie. Tel: +353 91 492838. Fax: +353 91 494520.

Running title

Lentiviral vectors in treatment of SCI

Abstract

Background

In this study we investigated the effect of Neurotrophin-3 (NT-3) and knockdown of NG2, one of the main inhibitory chondroitin sulphate proteoglycans (CSPGs), in the glial scar following spinal cord injury (SCI).

Methods

Short hairpin RNAs (shRNAs) were designed to target NG2 and were cloned into a lentiviral vector (LV). A LV was also constructed containing NT-3. LVs expressing NT-3, shRNA to NG2 or combinations of both vectors were directly injected into contused rat spinal cords one week post injury. Six weeks post injection of LVs spinal cords were examined by histology for changes in scar size and by immunohistochemistry for changes in expression of CSPGs, NT-3, astrocytes, neurons and microglia/macrophages. Motor function was assessed using Basso, Beattie and Bresnahan (BBB) locomotor scale.

Results

Animals that received the combination treatment of LV shNG2 and LV NT-3 showed reduced scar size. These animals also showed an increase in levels of neurons and NG2, a decrease in levels of astrocytes and also showed significant functional recovery as assessed using the BBB locomotor scale at 2 weeks post treatment.

Discussion

The improvement in locomotor recovery and decrease in scar size shows the potential of this gene therapy approach as a therapeutic treatment for SCI.

Key Words

astrocytes, axon regeneration, CSPGs, glial scar, microglia, NG2, NT-3, spinal cord injury.

Abbreviations

AEC	3-Amino-9-ethylcarbazole
ANOVA	analysis of variance
BBB	Basso, Beattie Bresnahan
chABC	chondroitinase ABC
CSPG	chondroitin sulphate proteoglycan
ECM	extracellular matrix
GAG	glycosaminoglycan
GFAP	glial fibrillary acidic protein
GFP	green fluorescent protein
IP	intraperitoneal
LV	lentiviral vector
NGS	normal goat serum
NT-3	neurotrophin-3
OPCs	oligodendrocytes precursor cells
P	probability value
PBSA	phosphate buffered saline containing 1% albumin
SCI	spinal cord injury

shRNAs short hairpin RNAs

Vv volume fraction

Introduction

Following SCI the CNS fails to regenerate, resulting in permanent paralysis for many patients. The failure of the CNS to regenerate can be attributed to both a lack of trophic support for regenerating axons, and inhibitory factors which are upregulated following injury to the CNS (1-4)

One of the main inhibitory hurdles which needs to be overcome to allow regeneration is the glial scar, which forms at the lesion site following injury (5). The glial scar predominately consists of astrocytes, oligodendrocyte precursor cells (OPCs) and microglia (6). These cells migrate to the site of injury and form a dense scar-like structure which acts as a physical barrier to neuron regeneration. The cells of the glial scar also upregulate the production of inhibitory molecules. CSPGs are one of the main groups of inhibitory molecules (7). CSPGs are a family of extracellular matrix (ECM) molecules, which are comprised of a core protein surrounded by a variable amount of repeating sulphated glycosaminoglycan (GAG) side chains. It is widely believed that the repeating GAG side chains are responsible for the inhibitory effect of CSPGs, as the removal of these side chains by enzymatic digestion reverses the inhibitory effect of CSPGs (8, 9). CSPGs are upregulated by reactive astrocytes and OPCs. The main members of the CSPG family are aggrecan, versican, neurocan, brevican, phosphacan and NG2. NG2 is one of the main inhibitory CSPGs upregulated following injury to the CNS (10). The inhibitory effect of NG2 has been well documented *in vitro*, where it has been shown that axons will avoid NG2 rich areas and that NG2 induces growth cone collapse (11). The inhibitory effect of NG2 following SCI has been confirmed by the use of a blocking antibody, which resulted in improved regeneration (12). The removal of NG2 GAG side chains, by digestion with the enzyme chondroitinase ABC (chABC), showed locomotor recovery and regeneration of sensory axons (9).

Reduction of NG2 levels through various mechanisms offers a potential therapy for overcoming the inhibitory environment of the glial scar.

Several papers contradict the non-permissive nature of CSPGs, where axons have been shown to extend into cellular grafts placed into the spinal cord lesion sites despite CSPG upregulation at the lesion site (13, 14). Although it has been suggested that the absence of NG2 enhances axonal regeneration in the CNS, it has also been shown that the absence of NG2 has no effect on regenerative growth of dorsal root axons into the spinal cord after dorsal root injury. In addition, it has been shown that absence of NG2 has no effect on sensory or motor axons within the spinal cord following spinal cord injury in NG2 knockout mice (15). Robust and sustained axon growth into spinal cord lesions have been noted, many of which were located along NG2 profiles (16).

RNA interference, in the form of viral delivery of shRNA, has shown positive effects in treatment of various neurodegenerative diseases such as Alzheimer's disease and Huntington's disease (17, 18). In a recent study, we showed that shRNA delivery by lentiviral vectors reduce levels of NG2 in the inhibitory Neu7 astrocyte cell line (19). The use of shRNA offers the potential of specifically targeting individual CSPGs. In addition the use of a lentiviral vector to deliver shRNA can provide long term expression of the shRNA, reducing the need for repeat administrations, such as those required with chABC and blocking antibodies.

NT-3 is a potent trophic factor for axonal growth, axonal pathfinding and in the development of sensory axons (20-22). There is already quite a substantial body of work in the literature on the potential therapeutic applications of NT-3 (23-26). NT-3 has been reported to have a regenerative effect on injured spinal cord (27, 28). Viral vectors have been used to regenerating axons with NT-3 (23, 29) demonstrating the huge potential of NT-3 as a guidance factor post SCI. Importantly for functional recovery, NT-3 can promote regrowth of corticospinal axons (29, 30).

Direct injection of therapeutics has proven a highly successful method for the delivery to the CNS. A single injection of chABC has been shown to be sufficient to provide long term changes in the ECM following SCI, up to 8 weeks post direct injection (31). In this study we propose that the direct injection of lentiviral vectors, encoding NT-3 and/or a shRNA to NG2, into the contused rat spinal cord will contribute to axonal regeneration and functional recovery.

Methods

Lentiviral vector production

Lentiviral vectors LV green fluorescent protein (GFP), LV shNG2 and LV NT-3 were produced and titered as previously described in Donnelly et al. (19). A siRNA was designed against NG2 and this was cloned into the pLVTHM lentiviral expression plasmid under the control of the H1 promoter. A siRNA scramble, was also designed as a control. The siRNA sequence that was used to construct the shRNA is as follows: sense- 5'CGAGUGAGGUACCUGAGUAUU 3' anti-sense- 5' UACACAGGUACCUCACUCGAA 3'. The shRNA was cloned into a pSUPER vector, from this the shRNA was cloned into pLVTHM at the BamH1 and Mlu1 sites. (pLVTHM shNG2), which also contains GFP as a marker gene. The pWPT expression plasmid was modified by replacing the GFP gene with the human NT-3 gene. Lentiviral vectors were produced using Jet PEI transfection reagent (Autogen Bioclear UK Ltd, Wiltshire, UK) according to manufacturers' protocol. Virus was harvested 48 and 72h post transfection and concentrated by ultracentrifugation at 27,000g for 2.5 hrs. Virus was aliquoted and stored at -80°C. Fixed volumes of the virus were used to transduce HeLa cells. Quantitative PCR was performed on the HeLa DNA for the viral GAG gene to determine viral titre. The following primers for GAG were used: forward 5' GGAGCTAGAACGATTCGCAGTTA 3'; reverse: 5'

GGTTGTAGCTGTCCCAGTATTTGTA 3'. All quantitative real time PCR was performed on the ABI onestep machine (Applied Biosystems, Foster City, CA, USA), on the standard programme, using beta actin as a control gene.

Spinal cord injury

All procedures performed were conducted under an animal license and were approved by an Animal Care and Research Ethics Committee. Spinal cord contusion injuries were performed using an Infinite Horizon impactor device (Precision Systems and Instrumentation, Lexington, KY, USA). Fifty female Sprague Dawley rats (weighing approximately 250g) were anaesthetised by intraperitoneal (IP) injection of ketamine and xylazine (100mg/kg and 10mg/kg respectively) and shaved at the cervical region of the back of the spine. Gel tears ointment was applied for eye protection. Rats were kept warm on a heating pad during surgery. The site of incision was shaved and disinfected with Betadine. A 2 inch incision was made on the dorsal aspect of the spine from T7-T10. After dissecting fascia and muscles on the dorsal spinous processes, laminectomy was performed at the T8-T10 level and dorsum of the spinal cord was exposed. A moderate contusion injury was introduced using the IH impactor device at 200 kilodyne. Following injury, the muscle and skin above the exposed spinal cord were sutured. Animals were housed separately overnight on a heating pad.

Acute post-operative care included careful monitoring of body temperature and use of heat lamps or heating pads as necessary. Post-operative care included twice daily monitoring for wound sepsis and bladder expression. Animals exhibiting signs of paralysis were monitored. Bladder expressions were performed on an as needed basis as determined by clinical palpation exam. Antibiotics were administered for one week following surgery or as deemed necessary. Analgesia was administered twice a day for one week post surgery or as deemed necessary.

Viral vector injection

Six days following contusion injury the animals were assessed for inclusion in the study, using the BBB locomotor scale (described below). Animals were randomly assigned to the following experimental groups; Phosphate buffered saline containing 1% albumin (PBSA) vehicle, LV NT-3, LV shNG2 and LVshNG2 + LV NT-3. Included animals were anaesthetised with Isoflurane. The site of injury was exposed as described above. The animals were secured beneath a stereotaxic frame. Vehicle/Virus was delivered using bevelled glass pipette tips attached to 33G Hamilton microsyringes. A volume of 1µl was injected 2mm rostral and 2mm caudal to the injury site, at a depth of 1.5mm from the dorsal surface of the spinal cord. A time lapse of 5 minutes was allowed after injection before removing the needle to prevent leakage of the vehicle/virus. Following injection, the muscle and skin above the exposed spinal cord was sutured. Post-operative care was provided as outlined above. Six weeks following injection animals were sacrificed by sodium pentobarbitone overdose. Animals were perfused transcardially with 4% paraformaldehyde containing 30% sucrose. The spinal column was removed and post-fixed for 5 days. The spinal cord was dissected from the spinal column. A 2cm segment of the spinal cord, including the lesion, was removed and stored in 30% sucrose in PBS at 4°C for up to two weeks. Spinal cords were snap frozen in liquid nitrogen chilled isopentane and stored at -80°C. Spinal cords were mounted in OTC mounting medium and sectioned longitudinally into 20µm thick cryostat sections. After mortality the n numbers for the experimental groups were: PBSA (n=8), LV NT-3 (n=9), LV shNG2 (n=8), LV shNG2 + LV NT-3 (n=8).

BBB behavioural analysis

Animals were placed in a Perspex box and allowed to move freely around the box for 3 minutes. The animals' movements were observed and noted by two blinded observers. The animals were then given a score from the 21 point BBB scale according to the movement

which was recorded. Open field testing was performed the day prior to viral injection, for inclusion in the study. BBB point of 14 or higher was selected as the point for excluding animals from the study. Included animals were then tested 2, 4 and 6 weeks post vehicle/viral vector injection. A one way analysis of variance (ANOVA) was carried out using Minitab software and post-hoc comparisons were undertaken by Tukey's post hoc test. Differences were considered to be statistically significant at probability value (P) < 0.05.

Sirius red histological staining

Tissue sections were allowed to rehydrate for 20 minutes in 1X PBS. Slides were then incubated in tap water for 5 minutes, to remove traces of OCT. Slides were incubated in Mayer's Hematoxylin for 5 minutes, to visualize nuclei. Hematoxylin was removed by slowly running tap water for 5 minutes. Slides were incubated in Picric acid-Sirius red solution for 1 hour and washed in acidified water. Slides were dehydrated through graded alcohol changes, incubated in xylene and mounted in DPX.

Immunohistochemical staining

Immunohistochemistry for detection of NT-3 and the CSPGs NG2 and neurocan was carried out using a 3-Amino-9-ethylcarbazole (AEC) chromagen detection kit (Sigma-Aldrich) to detect these antigens using light microscopy. Tissue sections were allowed to rehydrate as above and were incubated in 1% hydrogen peroxide in methanol solution for 20 minutes. Sections were washed in 1X PBS and blocked with 5% normal goat serum (NGS; Sigma-Aldrich, Ireland) blocking buffer for 20 minutes. The primary antibodies Rabbit IgG NT-3 (Chemicon), Mouse IgG NG2 (Zymed) and Mouse IgG neurocan (Millipore) were diluted 1:100 in blocking buffer and incubated with the sections for 1.5 hours. The primary antibodies were removed, followed by three 1X PBS washes and the horseradish peroxidase conjugated secondary antibody (Sigma-Aldrich; diluted 1:50 in blocking buffer) for 30

minutes. Secondary antibody was removed, sections were washed as above and incubated in Strept-avidin (Sigma-Aldrich; diluted 1:20 in 1X PBS) for 30 minutes. Sections were washed and incubated with AEC chromogen for 14 minutes. Sections were washed and incubated in Mayer's hematoxylin for 20 seconds, followed by wash in tap water. Sections were mounted in Aquatex aqueous mounting medium (Harleco).

For detection of dual Immunohistochemical labelling, fluorescent immunohistochemistry was carried out using the protocol below. Tissue sections were allowed to rehydrate as above and were then incubated with 20% NGS in 1X PBS containing 0.2% Triton-X for 20 minutes. The primary antibodies Mouse IgG β -III tubulin (Chemicon), Rabbit IgG Glial fibrillary acidic protein (GFAP; DakoCytomation), Mouse IgG CD11b (Chemicon), Rabbit IgG IBA1 (Wako), Mouse IgG NG2 (Zymed) and Mouse IgG neurocan (Millipore) were diluted 1:100 in 1X PBS containing 0.02% Triton-X and incubated with the sections for 2 hours at room temperature. Primary antibodies were removed and sections washed in 1X PBS. The secondary antibodies anti-Mouse rhodamine (Sigma-Aldrich) and anti-Rabbit fluorescein (Sigma-Aldrich) were diluted (1:100) in 1X PBS and added to the sections for 1 hour at room temperature in darkness. Secondary antibodies were removed and sections washed with 1X PBS. DAPI (Sigma-Aldrich) was used to stain cell nuclei. A 1 μ g/ml solution of DAPI was added to the sections for 5 minutes. After washing, sections were mounted with a drop of Fluoromount mounting media (Dakocytomation). In each experiment a negative control was carried out whereby the primary antibody was replaced with buffer.

Stereology

Scar size

The size of the glial scar surrounding the lesion was examined using stereological methods by a blinded experimenter. Scar tissue was defined as the tissue staining red with Sirius red. Three images were captured from five animals within each of the four experimental group and

also in a viral control group (LV GFP) using a 1.25X objective lens using an Olympus IX81 light microscope. Images were taken to include the lesion site. Equivalent slides were compared between animals from each experimental group. Estimation of scar volume was carried out using the Cavalieri method. A point grid was randomly placed onto images of spinal cord sections. All points hitting spinal cord tissue, scar and artifact were counted and recorded. Volume of scar was calculated for each experimental group using the following formula,

$$V = \sum P \cdot A \cdot T$$

That is, V=Volume, P= Number of points hitting region of interest, A=Area associated with each point and T=Distance between each sampled section,

Where,

Area associated with each point = (Distance between adjacent points/Linear Magnification)².

Cellular environment at lesion site

Stereological analysis was also carried out by a blinded experimenter on immunostained spinal cord sections within each of the four experimental groups to determine the proportion of cells at the lesion site that were immunoreactive for markers of CSPGs (NG2 positive / neurocan positive), NT-3, astrocytes (GFAP positive), neurons (β -III tubulin positive), microglia/macrophages (CD11b positive), i.e. the volume fraction (V_v) of immunoreactive cells at the lesion site. For each antibody, 4 images were captured per section using a 20X objective lens on an Olympus IX81 structured light microscope. The images were captured at random from fields of view around the edge of the lesion from five animals within each experimental group. These images were captured such that the edge of the lesion containing the cyst was bordering on either the top or bottom of the image. A point grid was again placed randomly on the images captured and the number of points hitting immunoreactive structures and the entire field of view were counted and recorded in Microsoft Excel. V_v of

the immunoreactive tissue was calculated by dividing the number of points overlying immunoreactive cells by the total number of points hitting tissue. Mean Vv immunoreactivity \pm SE was calculated for the experimental groups.

Statistical calculations for volume and Vv were performed using Minitab software. A one way ANOVA was carried out and post-hoc comparisons were undertaken by Tukey's post hoc test. Differences were considered to be statistically significant at $P < 0.05$.

Results

Histological analysis of scar

The scar size was assessed using sirius red staining in all experimental groups (Figure 1A-D). Interestingly in all treatment groups the scar size is reduced compared to the PBSA group, with the LV shNG2 + LV NT-3 group showing a significant reduction in scar size (Figure 1E). This was also true when scar size was examined in a viral control group injected with LV GFP (Supplementary figure 1). Potentially a thinner scar may offer less of a physical barrier to regeneration.

Analysis of cellular environment of lesion site

CSPGs – NG2 and neurocan

In order to assess the effect of the shRNA for NG2 in this model, slides from the centre of the lesion were immunohistochemically stained for detection of the CSPG NG2. Figure 2A-D shows representative images of NG2 immunohistochemistry within all experimental groups. Analysis of Vv of NG2 levels showed that NG2 appeared to increase across all experimental groups, peaking with a significant increase in NG2 in the LV shNG2 + LV NT-3 vector group compared with the PBSA vehicle group (Figure 2E).

In order to identify NG2 immunoreactive cells, dual staining for NG2 and IBA1 / GFAP was carried out. Supplementary figure 2A-E shows representative images of the NG2

and IBA1 dual staining in all experimental groups. Although a small number of IBA1 positive macrophages showed co-localization with NG2, especially in the LV NT-3 group, the majority of NG2 was not co-localized with IBA1. Supplementary figure 2 shows dual staining for NG2 and GFAP immunoreactive astrocytes. There were only low levels of co-localisation, suggesting that the NG2 positive cells may be OPCs and not reactive astrocytes.

In order to assess if the LV shNG2 is having an effect on the levels of other CSPGs, neurocan was chosen for immunohistochemical analysis. If NG2 levels are being altered, other CSPGs may possibly be upregulated to compensate for altered NG2 levels. Immunohistochemical analysis of neurocan in all experimental groups is shown in Figure 3A-D. Vv analysis of neurocan showed a trend toward an increase in neurocan levels in the experimental groups treated with LV shNG2, compared to the control groups (Figure 3E). It appeared that neurocan expression was mainly localized in cells within the lesion, these cells had a macrophage-like morphology. Dual immunohistochemical staining was carried out for neurocan and IBA1 (Supplementary figure 3). IBA1 staining confirmed that the large cells within the lesion were macrophages.

In order to determine that sufficient NT-3 was produced by LV NT-3, immunohistochemistry for NT-3 was carried out. Both groups that received LV NT-3 showed a trend (although not significant) towards increased NT-3 Vv compared to the PBSA group (Supplementary figure 4).

Astrocytes

To assess if the experimental treatments can affect the levels of reactive astrocytes, sections were stained for GFAP. Figure 4A-D shows representative images for GFAP immunohistochemistry in all experimental groups. There appeared to be less GFAP in both experimental groups that received LV shNG2 (Figure 4E). This may suggest that the shRNA NG2 is reducing the proportion of astrocytes within the tissue.

Neurons

Immunohistochemistry was carried out for β -III tubulin to examine the effect of experimental treatments on neurons at the lesion site. Figure 5A-D shows representative staining for β -III tubulin in all experimental groups. In this study the LV shNG2 + LV NT-3 group showed a slight increase in Vv β -III tubulin; however, this was not significant (Figure 5E).

Microglia / macrophages

CD11b was used here to assess the immune response following SCI. Figure 6A-D shows representative images of CD11b immunohistochemistry in all experimental groups. Vv analysis showed there was significantly less CD11b immunoreactivity in the group that received LV shNG2, when compared to the control group (Figure 6E).

Locomotor recovery

The BBB locomotor test was used to determine if functional recovery was observed following lentiviral treatment. Figure 7A shows locomotor function over the course of 6 weeks post injection of vehicle/viral vector. The percentage of improvement in BBB scores from inclusion to BBB analysis point over the 6 week period was calculated and is shown in Figure 7B. A significant improvement in BBB score was observed at 2 weeks in the LV shNG2 + LV NT-3 experimental group compared to the PBSA group (Figure 7B).

Discussion

In this study, we investigated the use of shRNA for NG2 and the over expression of NT-3 as a viable method to promote locomotor recovery and increase regeneration in a contusion model of SCI. As regeneration is a fine balance between permissive and inhibitory cues, neither the

reduction of the inhibitory environment nor providing neurotrophic factor alone will provide substantial regrowth (12, 32-33).

Here we demonstrated that there was an increase in NG2 levels in the experimental groups that received shRNA for NG2. If the cells which were originally transduced with the LV shNG2 substantially reduced NG2 levels, the surrounding non transduced cells may have increased their levels of NG2 production, to compensate for the initial reduction in NG2. The expression of neurocan shows a similar pattern to NG2 expression across the experimental groups at 6 weeks, which may suggest that a secondary migration of reactive astrocytes occurred (10). The hypothesis of the secondary migration of astrocytes, suggests that a second dose of viral vectors may be required at a later time point. Interestingly studies with NG2 knockout mice have shown that the absence of NG2 leads to less regeneration (34). This suggests that regeneration is a complex balance between repulsive and permissive cues (35). Complete removal of NG2 may not be desirable, and this is possibly the reason for the putative compensatory response of NG2 knockdown observed in this study.

There is clearly an increase in NT-3 expression in both the LV NT-3 and the LV shNG2 + NT-3 experimental groups, though this is not significant. These two experimental groups are also the groups which exhibit the highest levels of functional recovery compared to the other experimental groups at 2 weeks, which may be attributed to NT-3 promotion of corticospinal tract regeneration. The functional recovery in the three treatment groups is lowest in the LV shNG2 group, suggesting the increase in BBB score in the combined vector group may be due to NT-3 expression. The combined vector treatment group showed significantly higher % improvement in BBB score compared with the PBSA control group at 2 weeks. No such significant improvement was observed at 4 or 6 weeks, perhaps this is related to the aforementioned secondary migration of astrocytes into the lesion site. The functional recovery observed in this study may be contributed in part by NT-3 mediated regeneration of the corticospinal tract (29, 30). A study with a similar strategy to the present

study was carried out by Massey et al. (26), where chABC and lentiviral vectors expressing NT-3 were administered separately and in combination following SCI. In contrast to the results of our study, they found that when administered separately these treatments permitted a significant increase in axonal elongation. In the case of chABC, these effects may not be due to the inhibition of CSPGs but attributable to the growth promoting effects of the sulphated disaccharide units produced by the degradation of the GAG chains (36).

In our study the analysis of the cellular environment at the lesion site showed there was a trend increase in Vv of β III-tubulin in the LV shNG2 LV + NT-3 combination treated group compared to all groups. A point to note is, as the Vv of axons was calculated, the increase could be due to an increase in the number of axons or an increase in axon length or a combination of both factors. It may be possible that the other treatment groups contained spared axons and the combination treatment group had regenerating axons that moved into the perilesion area, as this is where a significant increase in axons was observed.

This study also explored how the treatments affected the proportion of astrocytes in the region around the lesion, as GFAP is upregulated in reactive astrocytes following SCI (36). Our results showed that both experimental groups that received LV shNG2 had significantly lower Vv of astrocytes. This indicates that the decrease in Vv of astrocytes to the perilesion region is attributable to a reduction in levels of NG2. As discussed above, CSPGs have adhesive properties and so can bind factors that affect cell activation and proliferation (37). It has been proposed that reactive gliosis is induced by factors such as thrombin, ciliary neurotrophic factor and interleukin-1 (38-40). NG2 may bind these, increasing their concentration locally, and so in the absence of NG2 these factors could diffuse and so would no longer be present in a high enough concentration to initiate gliosis.

Quantification of immune reaction was carried out by immunostaining for an antigenic marker found on microglial cells and macrophages (CD11b). Our results illustrate that only when the LV shNG2 experimental group showed a significant reduction in the immune

reaction in the perilesion area. As the combinatorial treatment did not have the same decrease in inflammatory levels as the LV shNG2 treated group it could also be postulated that NT-3 may even enhance the inflammatory reaction. It has been demonstrated *in vitro* that NT-3 promotes survival of microglia, stimulating proliferation and increasing phagocytic activity (41). When grafted into the injured spinal cord, microglia facilitate neurite extension (42). In contrast however, other studies have suggested that inflammation is the cause of the growth inhibitory environment that develops following SCI (43-44).

In summary, the combination treatment groups of LV shNG2 + LV NT-3 showed significant locomotor improvement at the two week time point. This LV shNG2 + NT-3 group showed a significantly thinner fibrotic scar size (as shown with sirius red staining), which may result in a reduced physical barrier to regeneration. Although not significant, the LV shNG2 + LV NT-3 group also showed a decrease in Vv GFAP and increase in Vv β -III tubulin, both of which are important factors in promoting regeneration. This study shows the potential of gene therapy as a therapeutic treatment for spinal cord injury

Acknowledgements

We wish to thank Professor Dider Trono (EFPL, Switzerland) for the kind gift of the lentiviral vector gene transfer and packaging plasmids. This work was supported by funding from the Health Research Board of Ireland and Science Foundation Ireland.

Declaration of interest

The authors report no conflicts of interest. The authors alone are responsible for the content and writing of the paper.

References

1. Dietz V, Curt A. Neurological aspects of spinal cord repair: promises and challenges. *Lancet Neurology*. 2006; 5: 688–94.
2. Houle JD, Tessler A. Repair of chronic spinal cord injury. *Experimental Neurology*. 2003; 182: 247–60.
3. Hulsebosch CE. Recent advances in pathophysiology and treatment of spinal cord injury. *Advances in Physiology Education*. 2002; 26: 238–55.
4. Zai LJ, Yoo S, Wrathall JR. Increased growth factor expression and cell proliferation after contusive spinal cord injury. *Brain Research*. 2005; 1052: 147–55.
5. Rudge JS, Silver J. Inhibition of neurite outgrowth on astroglial scars in vitro. *Journal of Neuroscience*. 1990; 10(11):3594-603.
6. Faulkner JR, Herrmann JE, Woo MJ, Tansey KE, Doan NB, Sofroniew MV. Reactive astrocytes protect tissue and preserve function after spinal cord injury. *Journal of Neuroscience*. 2004; 24(9):2143-55.
7. McKeon RJ, Schreiber RC, Rudge JS, Silver J. Reduction of neurite outgrowth in a model of glial scarring following CNS injury is correlated with the expression of inhibitory molecules on reactive astrocytes. *Journal of Neuroscience*. 1991; 11(11):3398-411.
8. Bradbury EJ, McMahon SB, Ramer MS. Keeping in touch: sensory neurone regeneration in the CNS. *Trends in Pharmacological Science*. 2000; 21(10):389-94.
9. Bradbury EJ, Moon LD, Popat RJ, King VR, Bennett GS, Patel PN et al. Chondroitinase ABC promotes functional recovery after spinal cord injury. *Nature*. 2002; 416(6881):636-40.,
10. Bu J, Akhtar N, Nishiyama A. Transient expression of the NG2 proteoglycan by a subpopulation of activated macrophages in an excitotoxic hippocampal lesion. *Glia*. 2001; 34(4):296-310.

11. Ughrin YM, Chen ZJ, Levine JM. Multiple regions of the NG2 proteoglycan inhibit neurite growth and induce growth cone collapse. *Journal of Neuroscience*. 2003; 23(1):175-86.
12. Tan AM, Colletti M, Rorai AT, Skene JH, Levine JM. Antibodies against the NG2 proteoglycan promote the regeneration of sensory axons within the dorsal columns of the spinal cord. *Journal of Neuroscience*. 2006; 26(18):4729-39.
13. Jones LL, Margolis RU, Tuszynski MH. The chondroitin sulfate proteoglycans neurocan, brevican, phosphacan and versican are differentially regulated following spinal cord injury. *Experimental Neurology*. 2003; 182: 399-411.
14. Jones LL, Sajed D, Tuszynski MH. Axonal regeneration through regions of chondroitin sulfate proteoglycan deposition after spinal cord injury: a balance of permissiveness and inhibition. *Journal of Neuroscience*. 2003; 23(28): 9276-88.
15. Hossain-Ibrahim MK, Rezajooi K, Stallcup WB, Lieberman AR, Anderson PN. Analysis of axonal regeneration in the central and peripheral nervous systems of the NG2-deficient mouse. *BMC Neuroscience*. 2007; 8(80): 1-22.
16. McTigue DM, Tripathi R, Wei P. NG2 colocalizes with axons and is expressed by a mixed cell population in spinal cord lesions. *Journal of Neuropathology and Experimental Neurology*. 2006; 65(4): 406-20.
17. Harper SQ, Staber PD, He X et al. RNA interference improves motor and neuropathological abnormalities in a Huntington's disease mouse model. *Proceedings of the National Academy of Sciences of the United States of America*. 2005; 102(16):5820-5.
18. Singer O, Marr RA, Rockenstein E. Targeting BACE1 with siRNAs ameliorates Alzheimer disease neuropathology in a transgenic model. *Nature Neuroscience*. 2005; 8(10):1343-9.

19. Donnelly EM, Strappe PM, McGinley LM et al. Lentiviral vector-mediated knockdown of the neuroglycan 2 proteoglycan or expression of neurotrophin-3 promotes neurite outgrowth in a cell culture model of the glial scar. *Journal of Gene Medicine*. 2010; 12(11): 863-72.
20. Tessarollo L, Tsoulfas P, Martin-Zanca D, Gilbert DJ, Jenkins NA, Copeland NG, Parada LF. trkC, a receptor for neurotrophin-3, is widely expressed in the developing nervous system and in non-neuronal tissues. *Development*. 1993; 118(2):463-75.
21. Williams R, Backstrom A, Kullander K, Hallbook F, Ebendal T. Developmentally regulated expression of mRNA for neurotrophin high-affinity (trk) receptors within chick trigeminal sensory neurons. *European Journal of Neuroscience*. 1995; 7(1):116-28.
22. Hari A, Djohar B, Skutella T, Montazeri S. Neurotrophins and extracellular matrix molecules modulate sensory axon outgrowth. *International Journal of Developmental Neuroscience*. 2004; 22(2):113-7.
23. Alto LT, Havton LA, Conner JM, Hollis li ER, Blesch A, Tuszynski MH. Chemotropic guidance facilitates axonal regeneration and synapse formation after spinal cord injury. *Nature Neuroscience*. 2009; 12(9):1106-13.
24. Grill R, Murai K, Blesch A, Gage FH, Tuszynski MH. Cellular delivery of neurotrophin-3 promotes corticospinal axonal growth and partial functional recovery after spinal cord injury. *Journal of Neuroscience*. 1997; 17(14):5560-72.
25. Hory-Lee F, Russell M, Lindsay RM, Frank E. Neurotrophin 3 supports the survival of developing muscle sensory neurons in culture. *Proceedings of the National Academy of Sciences of the United States of America*. 1993; 90(7):2613-7.
26. Massey JM, Amps J, Viapiano MS et al. Increased chondroitin sulfate proteoglycan expression in denervated brainstem targets following spinal cord injury creates a

- barrier to axonal regeneration overcome by chondroitinase ABC and neurotrophin-3. *Experimental Neurology*. 2008; 209(2):426-45.
27. Ramer MS, Bishop T, Dockery P et al. Neurotrophin-3-mediated regeneration and recovery of proprioception following dorsal rhizotomy. *Molecular and Cellular Neuroscience*. 2002; 19(2):239-49.
28. Zhou L, Baumgartner BJ, Hill-Felberg SJ, McGowen LR, Shine HD. Neurotrophin-3 expressed in situ induces axonal plasticity in the adult injured spinal cord. *Journal of Neuroscience*. 2003; 23(4):1424-31.
29. Blits B, Dijkhuizen PA, Boer GJ, Verhaagen J. Intercostal nerve implants transduced with an adenoviral vector encoding neurotrophin-3 promote regrowth of injured rat corticospinal tract fibers and improve hindlimb function. *Experimental Neurology*. 2000; 164(1):25-37.
30. Bradbury EJ, Khemani S, King VR, Priestly JV, McMahon SB. NT-3 promotes growth of lesioned adult rat sensory axons ascending in the dorsal columns of the spinal cord. *European Journal of Neuroscience*. 1999; 11(11):3873-83.
31. Galtrey CM, Asher RA, Nothias F, Fawcett JW. Promoting plasticity in the spinal cord with chondroitinase improves functional recovery after peripheral nerve repair. *Brain*. 2007; 130(4):926-39.
32. Ikegami T, Nakamura M, Yamane J et al. Chondroitinase ABC combined with neural stem/progenitor cell transplantation enhances graft cell migration and outgrowth of growth-associated protein-43-positive fibers after rat spinal cord injury. *European Journal of Neuroscience*. 2005; 22(12):3036-46.
33. Schnell L, Schneider R, Kolbeck R, Barde Y-A, Schwab ME. Neurotrophin-3 enhances sprouting of corticospinal tract during development and after adult spinal cord lesion. *Nature*. 1994; 367(6459):170-3.

34. de Castro R, Jr., Tajrishi R, Claros J, Stallcup WB. Differential responses of spinal axons to transection: influence of the NG2 proteoglycan. *Experimental Neurology*. 2005; 192(2):299-309.
35. Jones LL, Sajed D, Tuszynski MH. Axonal regeneration through regions of chondroitin sulfate proteoglycan deposition after spinal cord injury: a balance of permissiveness and inhibition. *Journal of Neuroscience*. 2003; 23(28):9276-88.
36. Silver J, Miller JH. Regeneration beyond the glial scar. *Nature Reviews Neuroscience*. 2004; 5(2):146-56.
37. Rolls A, Shechter R, Schwartz M. The bright side of the glial scar in CNS repair. *Nature Reviews Neuroscience*. 2009; 10(3):235-41.
38. Giulian D, Woodward J, Young D, Krebs J, Lachman L. Interleukin-1 injected into mammalian brain stimulates astrogliosis and neovascularization. *Journal of Neuroscience*. 1988; 8(7):2485-90.
39. Nishino A, Suzuki M, Ohtani H, Motohashi O, Umezawa K, Nagura H, Yoshimoto T. Thrombin May Contribute to the Pathophysiology of Central Nervous System Injury. *Journal of Neurotrauma*. 1993; 10(2):167-79.
40. Winter CG, Saotome Y, Levison SW, Hirsh D. A role for ciliary neurotrophic factor as an inducer of reactive gliosis, the glial response to central nervous system injury. *Proceedings of the National Academy of Sciences of the United States of America*. 1995; 92(13):5865-9.
41. Elkabes S, DiCicco-Bloom E, Black I. Brain microglia/macrophages express neurotrophins that selectively regulate microglial proliferation and function. *Journal of Neuroscience*. 1996; 16(8):2508-21.
42. Rabchevsky AG, Streit WJ. Role of microglia in postinjury repair and regeneration of the CNS. *Mental Retardation and Developmental Disabilities Research Reviews*. 1998; 4(3):187-92.

43. Fitch MT, Doller C, Combs CK, Landreth GE, Silver J. Cellular and Molecular Mechanisms of Glial Scarring and Progressive Cavitation: In Vivo and In Vitro Analysis of Inflammation-Induced Secondary Injury after CNS Trauma. *Journal of Neuroscience*. 1999; 19(19):8182-98.
44. Fitch MT, Silver J. Activated Macrophages and the Blood-Brain Barrier: Inflammation after CNS Injury Leads to Increases in Putative Inhibitory Molecules. *Experimental Neurology*. 1997; 148(2):587-603.

Figure legends

Figure 1

Photomicrographs show sirius red staining in experimental groups treated with (A) PBSA, (B) LV NT-3, (C) LV shNG2 and (D) LV shNG2 + LV NT-3. Scalebar = 1mm. Double headed arrow in (D) shows lesion, single arrow shows scar. Graph shows the volume of the scar (E). Mean \pm SEM. *= $p < 0.05$, Tukey's post hoc test using One way ANOVA.

Figure 2

Photomicrographs show NG2 immunohistochemistry within the edge of the lesion in experimental groups treated with (A) PBSA, (B) LV NT-3, (C) LV shNG2 and (D) LV shNG2 + LV NT-3. Scalebar = 50 μ m. (E) Graph shows Vv of NG2 in the glial scar. Mean \pm SEM. *= $p < 0.05$, Tukey's post hoc test using One way ANOVA

Figure 3

Photomicrographs show neurocan immunohistochemistry within the edge of the lesion in experimental groups treated with (A) PBSA, (B) LV NT-3, (C) LV shNG2 and (D) LV shNG2 + LV NT-3. Scalebar = 50 μ m. (E) Graph shows Vv of neurocan at the lesion site. Mean \pm SEM.

Figure 4

Photomicrographs show GFAP immunohistochemistry within the edge of the lesion in experimental groups treated with (A) PBSA, (B) LV NT-3, (C) LV shNG2 and (D) LV shNG2 + LV NT-3. Scalebar = 50 μ m. (E) Graph shows Vv of GFAP at the lesion site. Mean \pm SEM. *= $p < 0.05$, Tukey's post hoc test using One way ANOVA.

Figure 5

Photomicrographs show β -III tubulin immunohistochemistry within the edge of the lesion in experimental groups treated with (A) PBSA, (B) LV NT-3, (C) LV shNG2 and (D) LV shNG2 + LV NT-3. Scalebar = 50 μ m. (E) Graph shows Vv of β -III tubulin at the lesion site. Mean \pm SEM. * = $p < 0.05$, Tukey's post hoc test using One way ANOVA.

Figure 6

Photomicrographs show CD11b immunohistochemistry within the edge of the lesion in experimental groups treated with (A) PBSA, , (B) LV NT-3, (C) LV shNG2 and (D) LV shNG2 + LV NT-3. Scalebar = 50 μ m. (E) Graph shows Vv of CD11b at the lesion site. Mean \pm SEM. * = $p < 0.05$, Tukey's post hoc test using One way ANOVA.

Figure 7

Graphs show (A) BBB locomotor scores with all experimental groups to 6 weeks post treatment, (B) Percentage of improvement in BBB scores to 6 weeks post treatment. Mean \pm SEM. * = $p < 0.05$, Tukey's post hoc test using One way ANOVA.

Supplementary Figure 1

Graph shows the volume of the scar in PBSA, LV NT-3, LV GFP, LV shNG2 and LV shNG2 + LV NT-3 animal groups. Mean \pm SEM. * = $p < 0.05$, Tukey's post hoc test using One way ANOVA.

Supplementary Figure 2

Photomicrographs show dual immunohistochemistry within the edge of the lesion for IBA1 (red) and NG2 (green) in all experimental groups (A,C,E,G) and dual immunohistochemistry for GFAP (green) and NG2 (red) in all experimental groups (B,D,F,H). DAPI staining shows

cell nuclei (blue). Animal groups: A-B=PBSA: C-D= LV NT-3: E-F= LV shNG2: G-H= LV shNG2 + NT-3. Scalebar=100 μ m.

Supplementary Figure 3

Photomicrographs show dual immunohistochemistry within the edge of the lesion for IBA1 (red) and neurocan (green) in experimental groups treated with (A) PBSA, (B) LV NT-3, (C) LV shNG2 and (D) LV shNG2 + LV NT-3. DAPI staining shows cell nuclei (blue). Scalebar=100 μ m.

Supplementary Figure 4

Photomicrographs show NT-3 immunohistochemistry within the edge of the lesion in experimental groups treated with (A) PBSA, (B) LV NT-3, (C) LV shNG2 and (D) LV shNG2 + LV NT-3. Scalebar = 50 μ m. (E) Graph shows Vv of NT-3 at the lesion site. Mean \pm SEM. *= p < 0.05, Tukey's post hoc test using One way ANOVA.

Figure 1

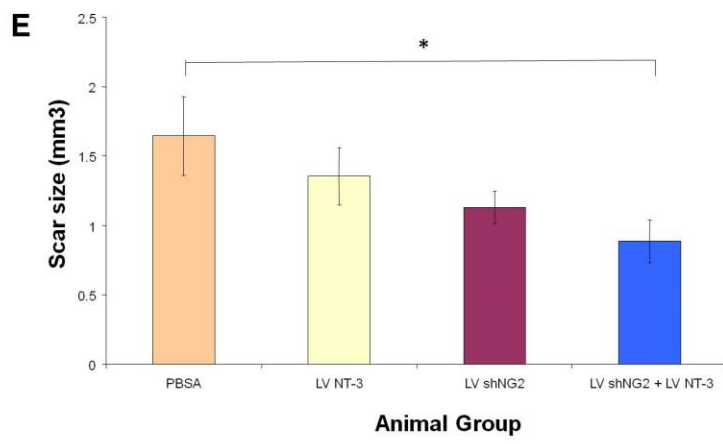
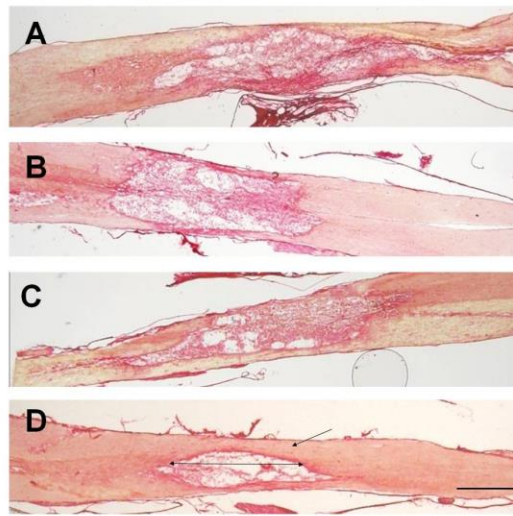


Figure 2

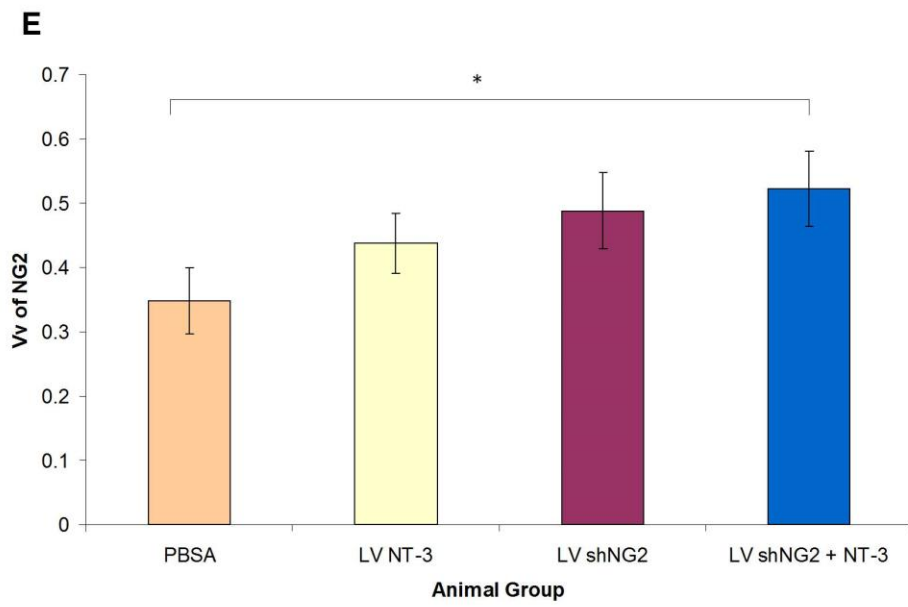
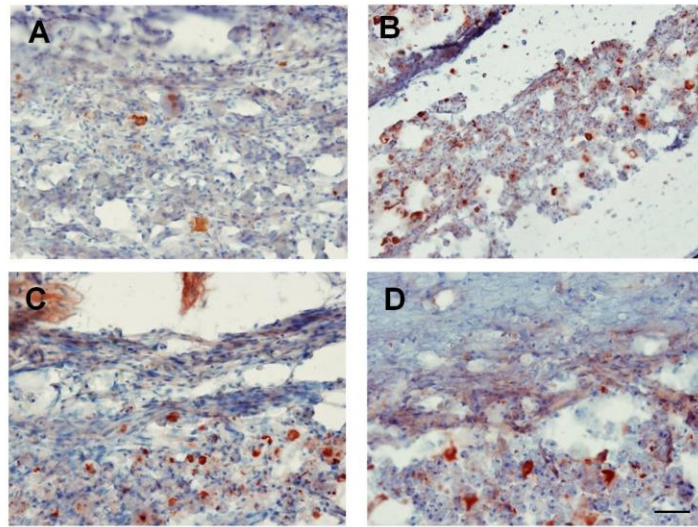


Figure 3

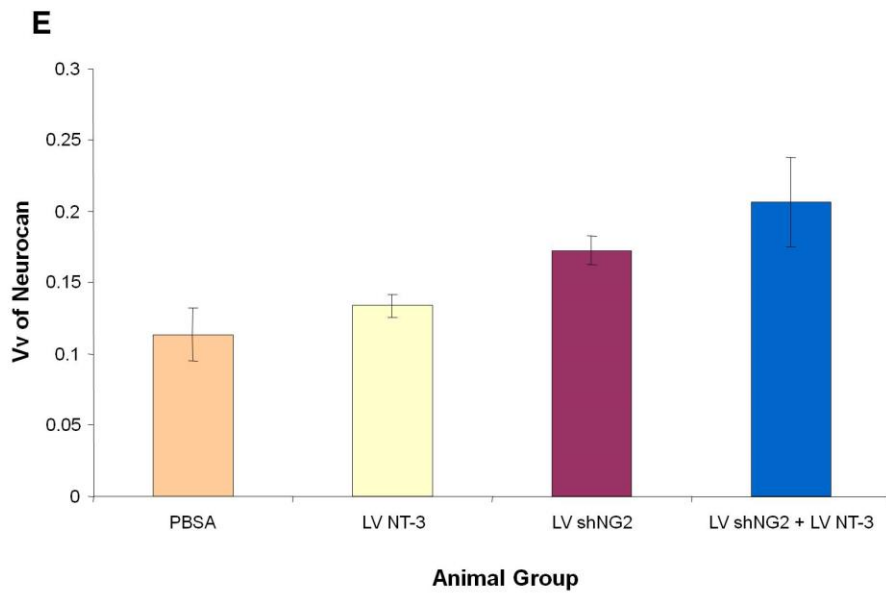
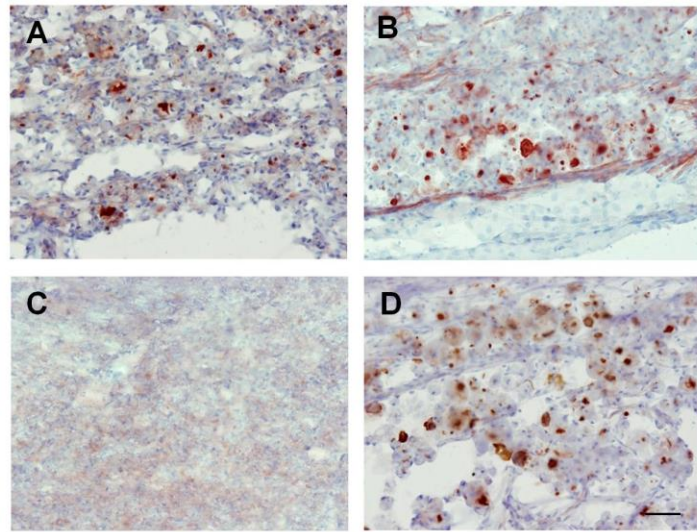


Figure 4

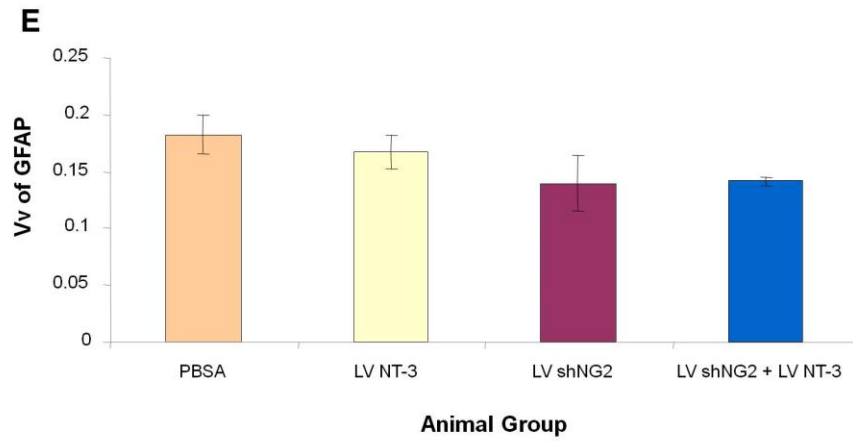
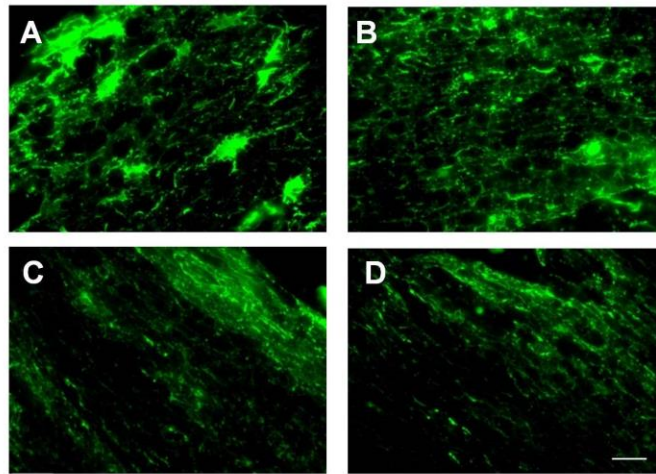


Figure 5

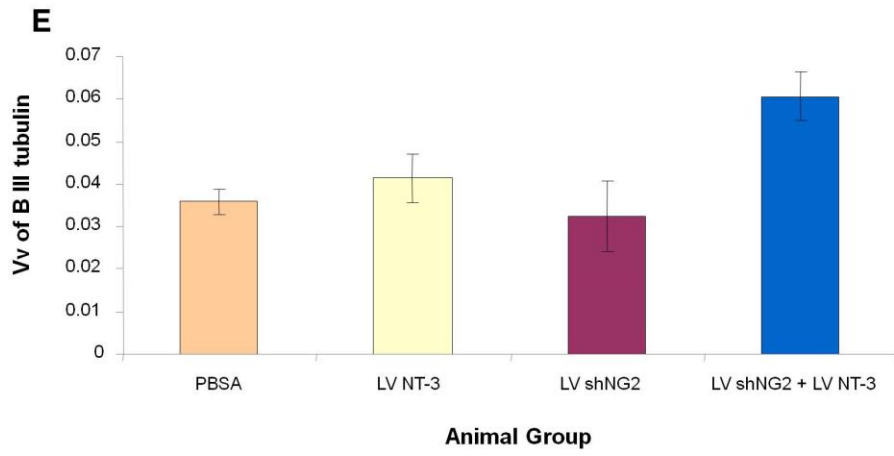
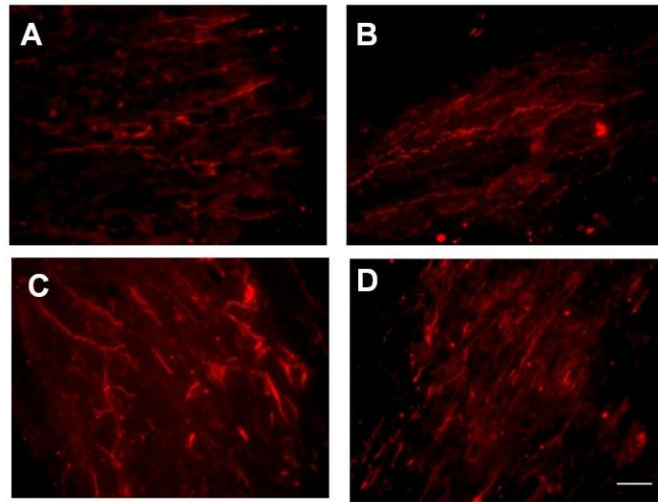


Figure 6

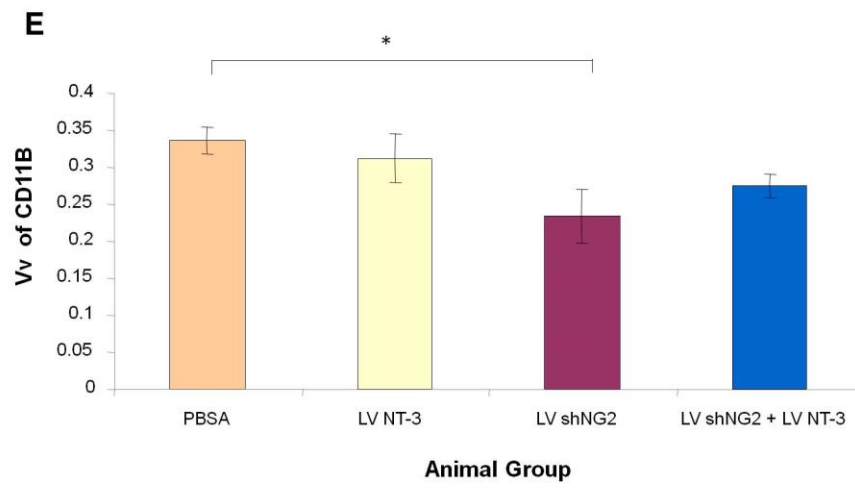
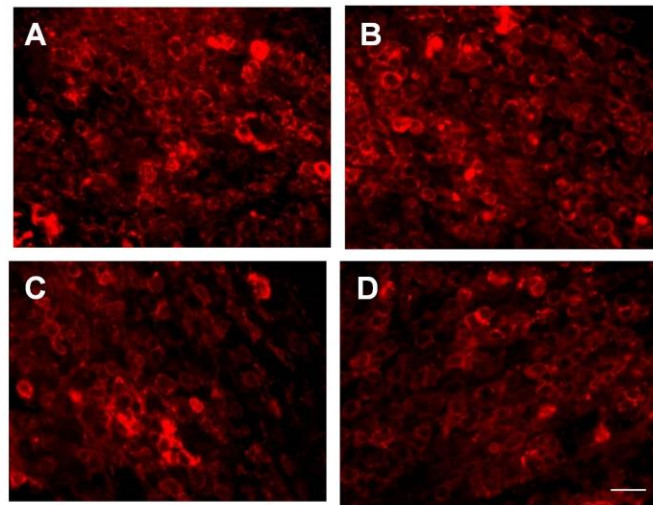
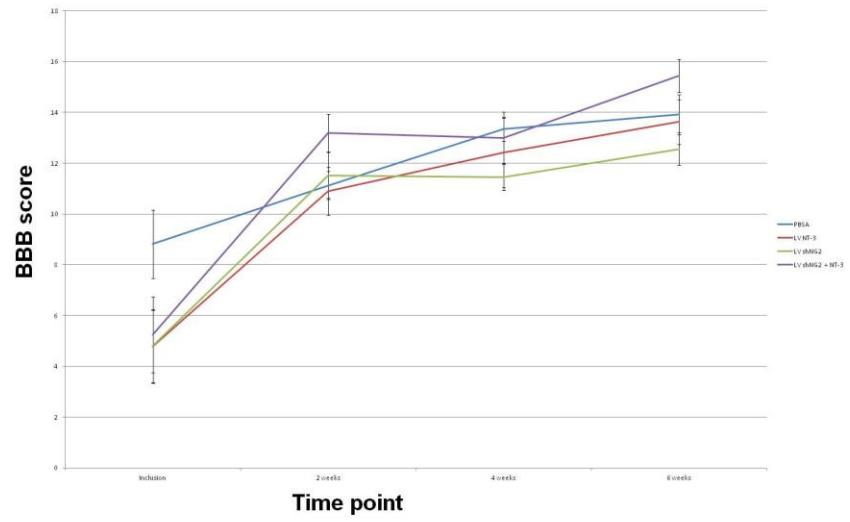
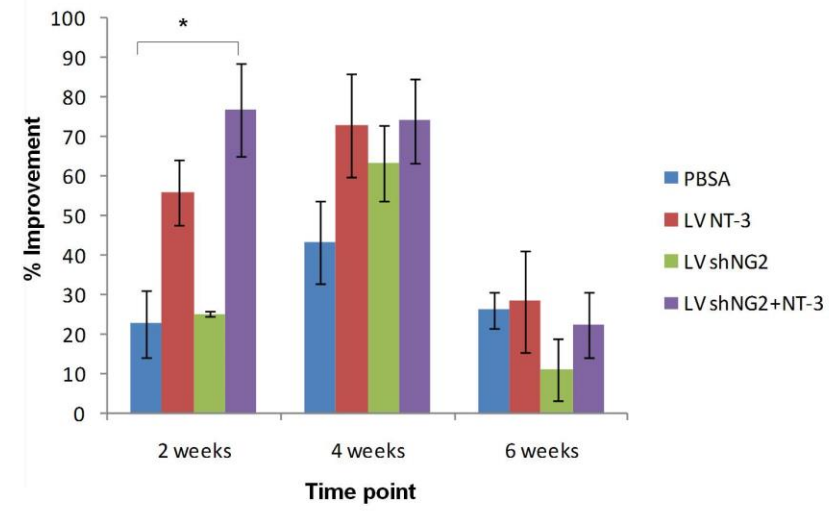


Figure 7

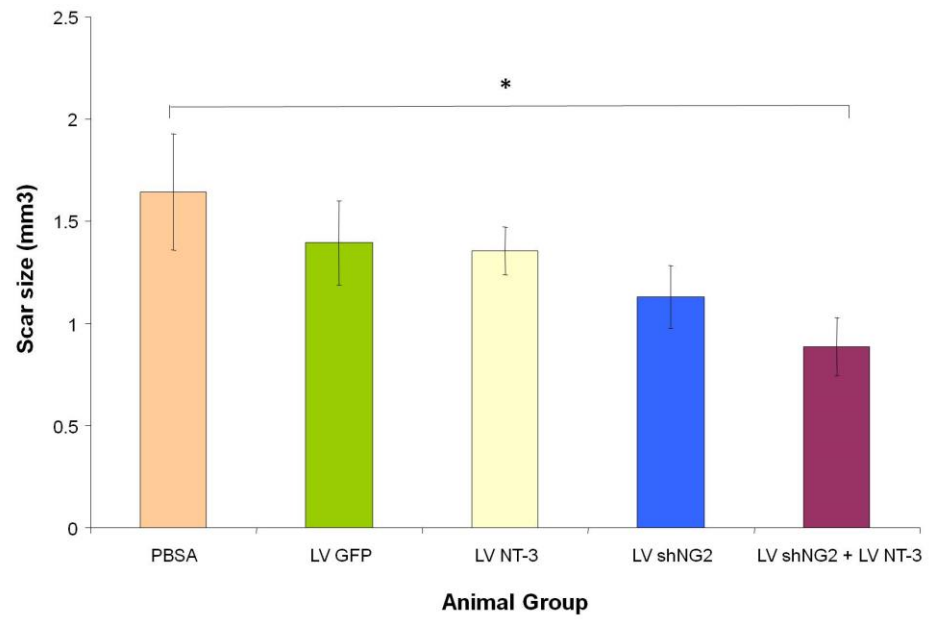
A



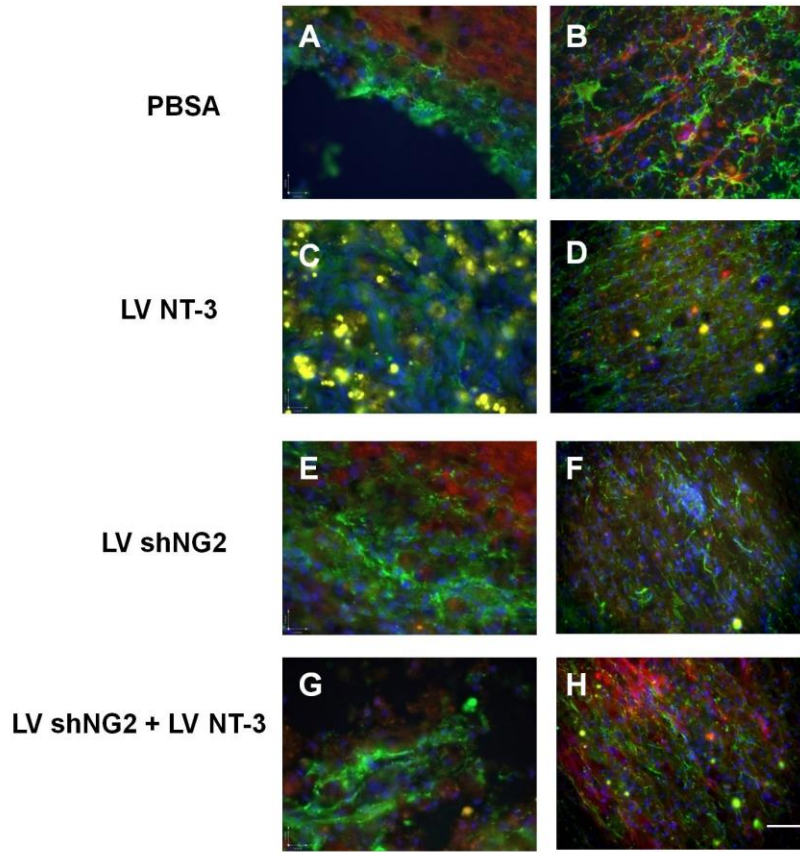
B



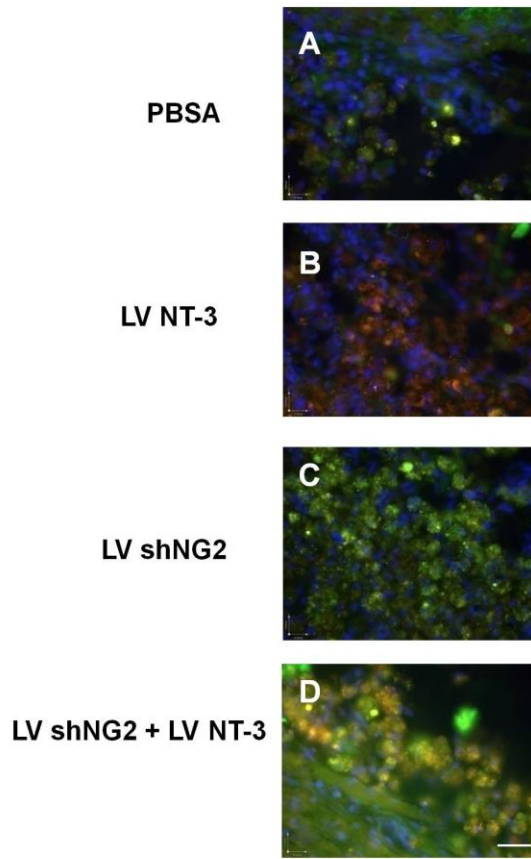
Supplementary Figure 1



Supplementary Figure 2



Supplementary Figure 3



Supplementary Figure 4

